THE JOURNAL OF PHYSICAL CHEMISTRY B

Article

pubs.acs.org/JPCB

From Formamide to Purine: An Energetically Viable Mechanistic Reaction Pathway

Jing Wang,[†] Jiande Gu,*[,†,‡] Minh Tho Nguyen,[§] Greg Springsteen,[∥] and Jerzy Leszczynski*[,†]

[†]Interdisciplinary Nanotoxicity Center, Department of Chemistry, Jackson State University, Jackson, Mississippi 39217, United States

[‡]Drug Design & Discovery Center, State Key Laboratory of Drug Research, Shanghai Institute of Materia Medica, Shanghai Institutes for Biological Sciences, CAS, Shanghai 201203, P. R. China

[§]Department of Chemistry, Katholieke Universiteit, Leuven, Belgium

[∥]Department of Chemistry, Furman University, 3300 Poinsett Highway, Greenville, South Carolina 29613, United States

Supporting Information

ABSTRACT: A step-by-step mechanistic pathway following the transformation of formamide to purine through a five-membered ring intermediate has been explored by density functional theory computations. The highlight of the mechanistic route detailed here is that the proposed pathway represents the simplest reaction pathway. All necessary reactants are generated from a single starting compound, formamide, through energetically viable reactions. Several important reaction steps are involved in this mechanistic route: formylation-dehydration, Leuckart reduction, five- and six-membered ring-closure, and deamination. On the basis of the study of noncatalytic pathways, catalytic water has been found to provide energetically viable step-by-step mechanistic pathways. Among these reaction steps, five-member ring-closure is the rate-determining step. The energy barrier (ca. 42 kcal/mol) of this rate-control step is somewhat lower than the rate-determining step (ca. 44 kcal/mol) for a pyrimidine-based pathway reported previously. The mechanistic pathway reported herein is less energetically demanding than for previously proposed routes to adenine.

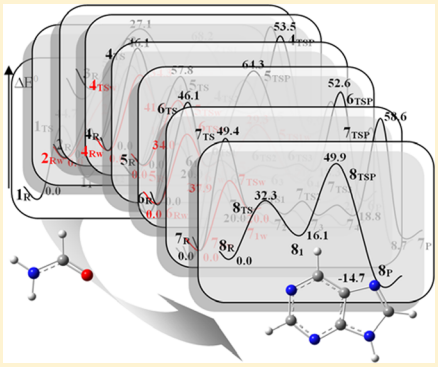

INTRODUCTION

The presence of biomolecules is the key for the development of life on earth. However, the origin of the primitive biomolecules such as nucleic bases remains an exciting, yet unsolved puzzle.[1−3] Numerous experiments demonstrated that the simple molecule, formamide ($HCONH_2$), is a potential abiotic source of nucleobases and their analogs.[4−7] Formamide dehydrates to HCN and water, thus providing all the essentials necessary for the synthesis of complex organics.[4,5,8] The synthesis of nucleobases in neat formamide has been explored experimentally.[4,5,9−17] Different mechanistic pathways yielding purines have been proposed, based on various experimental studies.[12−18] One suggested mechanistic route progresses through a pyrimidine intermediate to purine .[16,17] Also, a different route for the abiotic syntheses of both purine and adenine from formamide has been proposed from recent experimental investigation by the Springsteen group.[5] In this pathway, purine (or adenine) is formed through a five-membered ring intermediate, namely, 5-aminoimidazole (for purine) or 4-aminoimidazole-5-carboxamidine (AICN, for adenine).[5]

Parallel to experimental investigations, theoretical studies of reaction mechanisms are able to provide details about intermediates and transition states along the reaction pathway. Such information allows the selection of the most feasible route among various possible reaction pathways to be identified. However, finding a viable, thermodynamically realistic, step-by-step mechanism that can account for the formation of nucleobases is still a challenge for computational studies. A detailed computational investigation of step-by-step formation pathways from 4-aminoimidazole-5-carbonitrile (AICN) to adenine has been reported by the Schleyer group.[19] On the other hand, the density functional theory examination of the mechanistic pathway of the formation of adenine from formamide through pyrimidine has been performed by Sponer et al.[20] In these studies, HCN or CN anion has been adopted as a basic unit for the formation of adenine. However, computational investigations of the mechanisms of formamide have been limited only to basic chemical reactions.[8,21−23]

It is important to note that the mechanistic route proposed by the Springsteen group is highly similar to the biosynthesis of purine nucleobases.[24] It is this similarity between nucleobase abiotic syntheses and biosynthesis that stimulates our interests in exploring the step-by-step mechanism in the present study. Such investigations may provide a better elucidation of the origins of the metabolic pathway. As the first step, herein we report the step-by-step mechanistic pathways from formamide to purine based on a noncatalytic approach. We believe that this

Received: November 19, 2012
Revised: January 23, 2013
Published: January 24, 2013

   dx.doi.org/10.1021/jp311423q | J. Phys. Chem. B 2013, 117, 2314−2320

is an effective way to speculate on workable pathways accounting for the formation of these purine nucleobases. Subsequently, catalytic water was added to the investigations, in order to further probe energetically viable pathways.

COMPUTATIONAL METHODS

The studied models have been fully optimized by analytical gradient techniques. The density functional theory (DFT) with Becke's three parameter (B3)[25] exchange functional, along with the Lee–Yang–Parr (LYP)[26,27] nonlocal correlation functional (B3LYP), was applied in this study. The standard valence triple-ζ basis set, augmented by *d*-type polarization functions for heavy elements and *p*-type polarization functions for H, 6-311G(*d*,*p*),[28] was used. In the analysis of harmonic vibrational frequencies, the force constants were determined analytically for all of the complexes. The stationary structures are found by ascertaining that all of the harmonic frequencies are real. The corresponding transition states were characterized by the existence of single imaginary vibrational frequencies as the saddle points on the corresponding potential energy surface (PES). An intrinsic reaction coordinate (IRC) analysis was carried out to confirm that a transition state structure connects two corresponding minima. The polarizable continuum model (PCM) self-consistent reaction field of Tomasi and co-workers[29] was employed to evaluate the solvent effects (with a dielectric constant of 108.9 to mimic the solvent formamide) at the same calculation level. Our test computations of the main steps in the formation of HCN indicated that the corresponding activation energies (including the zero-point energy correction) predicted at the B3LYP/6-311G(d,p) level are close to those of the CCSD(T) predictions (with differences less than 2.5 kcal/mol). Therefore, the zero-point energy corrected energy profiles along the reaction pathways are expected to be satisfactory at the applied level of theory. All computations were performed using the Gaussian-09 package of programs.[30]

RESULTS

In addition to formamide, two more compounds, HCN and formate, are needed in the reaction route proposed by the Springsteen group.[5] As illustrated below, the former is a product of dehydration of formamide, while the latter is a result of hydrolysis of formamide. Therefore, this mechanistic route is exclusively based on formamide. Inclusion of the PCM model might be also important in some cases. However, in the present study, we find that the consideration of a solvent, at the PCM approximation, does not change the energy barriers significantly. This also can be seen from the previously reported studies by Schleyer's group,[19] in which the effects of solvent are less important for the reaction outcomes, especially when a large basis set is applied. Therefore, the discussion below is based on the results obtained in the gas-phase study.

1. Dehydration of Formamide: Formation of HCN. The mechanistic route of the dehydration of formamide has been explored at different levels of theory by Nguyen et al.[8] The main steps in the formation of HCN consist of the tautomerization of the amide form of formamide to its imidic acid form through an intramolecular proton transfer, followed by the loss of water (Figure 1). The activation energy (including the zero-point energy correction) of the tautomerization is calculated to be 44.7 kcal/mol (as shown as the energy profile in Figure 2) in the present DFT study. This

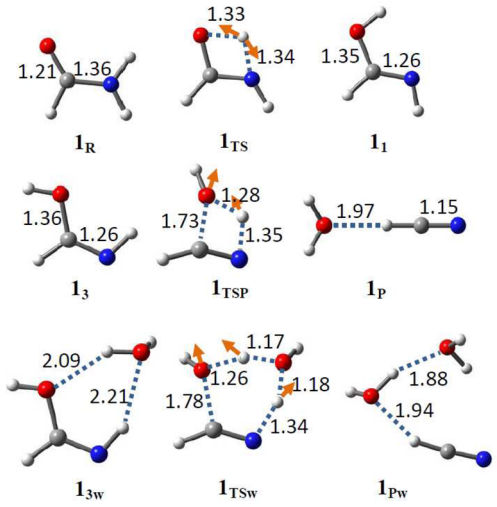

Figure 1. Optimized structures of the complexes involved in the dehydration of formamide as the local minima and the transition states on the potential energy surface at B3LYP/6-311G(d,p) level. Atomic distances are in Å. Orange arrows represent the vibrational mode corresponding to the single imaginary frequency in the transition states. Color representations are: red for oxygen, blue for nitrogen, gray for carbon, and white for hydrogen.

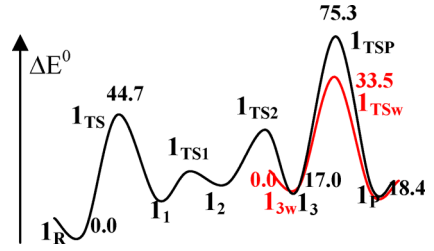

Figure 2. Schematic energy profile along the reaction pathway. ΔE^0 is the zero-point energy corrected relative energy (in kcal/mol). Black is for the noncatalyzed reaction. Red is for the water-catalyzed process.

energy barrier is slightly higher than the CCSD(T) prediction (42.3 kcal/mol) by Nguyen et al.[8] The energy barrier of the dehydration process obtained by the DFT study amounts to 58.3 kcal/mol, which is close to that predicted by CCSD(T) calculation (59.1 kcal/mol).[8] The zero-point energy corrected energy profiles along the reaction pathways are expected to be reasonable accurate. (The corresponding free energies are given in the Supporting Information.) Between these two main steps, there are two conformer rearrangement steps that have relatively lower energy barriers (see Supporting Information). The high energy barrier of the water-leaving step hinders the formation of HCN. However, this energy barrier (58.3 kcal/mol) is reduced to 33.5 kcal/mol when one water molecule is included. Intramolecular proton transfer in this case changes to an intermolecular proton transfer through the microsolvated water molecule (see Figure 1).

2. Formiminylation of HCN: Formation of 2-Iminoacetonitrile. Two steps have been identified in this reaction, that is, formylation and dehydration. In the first step (formylation), an intermediate product, 2-hydroxylaminoacetonitrile (2_1, see Figure 3), has been located as the local minimum structure on the PES. The carbon of CN anion attaches the carbon atom of the carbonyl group of formanide, forming a C—C single bond. Meanwhile, the proton of HCN in the reactants has transferred to the carbonyl oxygen, forming

dx.doi.org/10.1021/jp311423q | J. Phys. Chem. B 2013, 117, 2314–2320

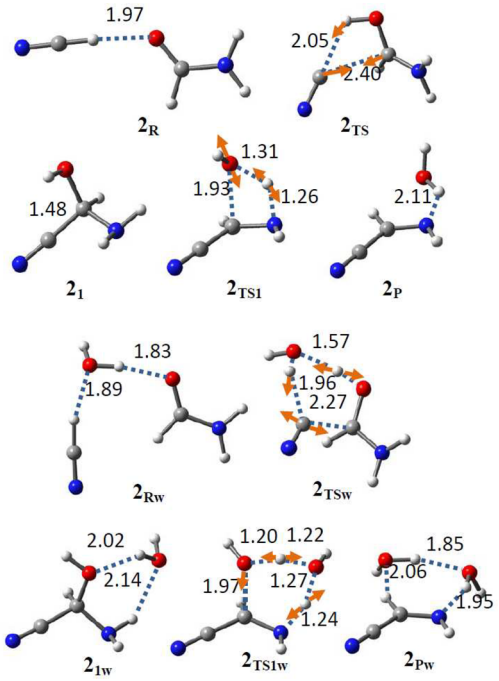

Figure 3. Optimized structures of the complexes as the local minima and the transition states on the potential energy surface in the formiminylation of HCN process at B3LYP/6-311G(d,p) level (atomic distance in Å). Orange arrows represent the vibrational mode corresponding to the single imaginary frequency in the transition states. Color representations are: red for oxygen, blue for nitrogen, gray for carbon, and white for hydrogen.

a hydroxyl group. The corresponding transition state structure ($\mathbf{2}_{TS}$, Figure 3) illustrates the formation of $\mathbf{2}_1$, 2-iminoacetonitrile, which is formed in the second step (dehydration). In this step, the hydroxyl group of the intermediate $\mathbf{2}_1$ interacts with the proton of the amino group, and subsequently leaves as a water molecule. This process has been shown in the corresponding transition state structure ($\mathbf{2}_{TS1}$) depicted in Figure 3. The energy profiles (Figure 4) of this reaction suggest

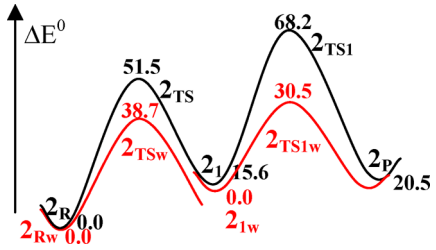

Figure 4. Schematic energy profile along the reaction pathway. ΔE^0 is the zero-point energy corrected relative energy (in kcal/mol). Black is for the noncatalyzed reaction. Red is for the water-catalyzed process.

that it is difficult to form $\mathbf{2}_1$ (with the activative energy barrier of 51.5 kcal/mol), even under high temperature, as reported in the experimental study.[5] Moreover, the energy barrier of 52.6 kcal/mol in the second step (dehydration) suggests that the dehydration process is unlikely to follow the simple route presented in Figure 4. Notice that due to the dehydration of formamide there are water molecules present in the reaction system. Therefore, one may consider that these newly formed water molecules could be involved in the reaction. With one microhydrated water molecule, we find that the activation energy of the formylation of HCN reduces to 38.7 kcal/mol while that of the dehydration of $\mathbf{2}_1$ reduces to 30.5 kcal/mol. The transition state structure depicted in Figure 3 demonstrates that a water molecule acts as a bridge for the proton transfer during these two reaction steps.

3. Leuckart Reduction:[31] Reduction of 2-Iminoacetonitrile to 2-Aminoacetonitrile. As a reducting agent, formate can be generated through hydrolysis of formamide by water. The activation energy of this reaction is 38.5 kcal/mol at the B3LYP/6-311G(d,p) level of theory (see Supporting Information). In the Leuckart reduction, a formate is found to provide two hydrogen atoms directly to the imino group of 2-iminoacetonitrile, yielding 2-aminoacetonitrile and carbon dioxide. The transition state structure ($\mathbf{3}_{TS}$) and the related local minimal structures depicted in Figure 5 reveal that the

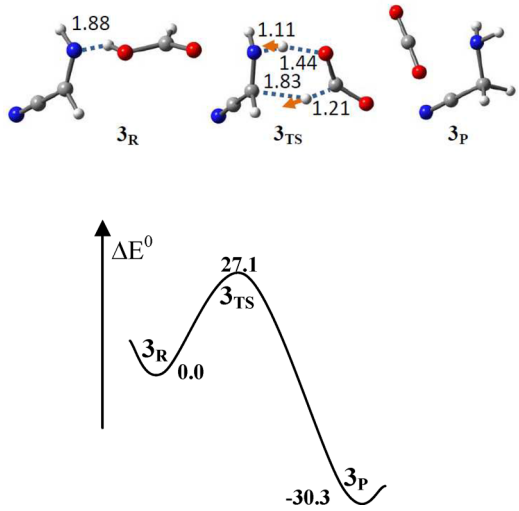

Figure 5. (Top) The optimized structures of the complexes as the local minima and the transition state on the potential energy surface in the Leuckart reduction, (atomic distance in Å). Orange arrows represent the vibrational mode corresponding to the single imaginary frequency in the transition states. Color representations are: red for oxygen, blue for nitrogen, gray for carbon, and white for hydrgen. (Bottom) Schematic energy profile along the reaction pathway. ΔE^0 is the zero-point energy corrected relative energy (in kcal/mol).

Leuckart reduction is an elementary reaction in this case. The activation energy of this reaction is evaluated to be 27.1 kcal/mol. The energy profile of the reaction route suggests that this reaction is irreversible; the energy barrier for the oxidation of 2-aminoacetonitrile amounts to 60.4 kcal/mol.

4. Formiminylation of 2-Aminoacetonitrile: The Formation of 2-Amidinoacetonitrile. Similar to the formiminylation of HCN, this reaction also consists of two main steps, formylation and dehydration. In the first step, one proton of the 2-amino group of 2-aminoacetonitrile migrates to the O atom of formamide, while the N atom of the deprotonated amino group of 2-aminoacetonitrile attaches to the carbon of the carbonyl group in formamide, forming an N—C single bond ($\mathbf{4}_1$). The structure of the corresponding transition state ($\mathbf{4}_{TS}$) demonstrates this process (Figure 6). A simple proton rotation around the C—O single bond follows, resulting in the formation of the conformer $\mathbf{4}_3$ (see Figure 6). The subsequent dehydration of $\mathbf{4}_3$ leads to the formation of 2-amidinoacetonitrile. In this step, the hydroxyl group of the intermediate $\mathbf{4}_3$ interacts with the proton of the secondary

dx.doi.org/10.1021/jp311423q | J. Phys. Chem. B 2013, 117, 2314−2320

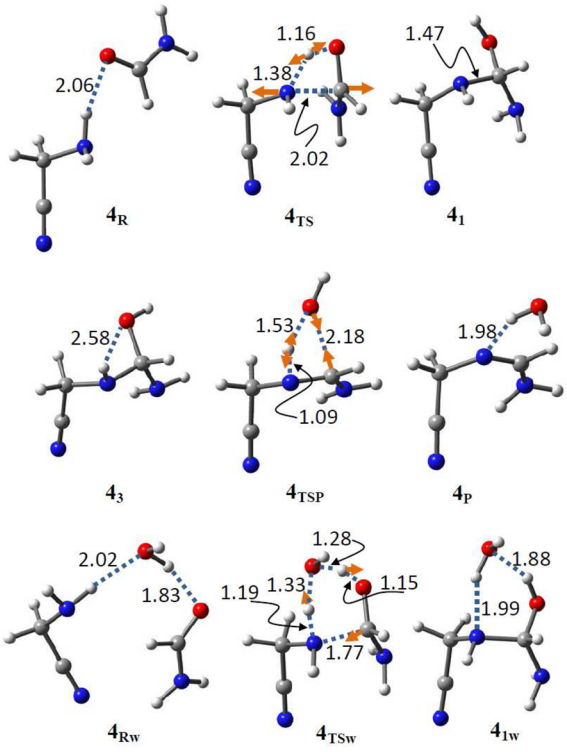

Figure 6. Optimized structures of the complexes as the local minima and the transition states on the PES in the process of formiminylation of 2-aminoacetonitrile (atomic distance in Å). Orange arrows represent the vibrational mode corresponding to the single imaginary frequency in the transition states. Color representations are: red for oxygen, blue for nitrogen, gray for carbon, and white for hydrogen.

amino group at the 2-position of the formylated 2-aminoacetonitrile, forming a water molecule as a leaving group. The corresponding transition state structure ($\mathbf{4}_{TSP}$) depicted in Figure 6 illustrates the dehydration process. The energy barrier of the formylation step in this reaction is high, about 46.1 kcal/mol (Figure 7). Similar to the formylation of HCN, when a

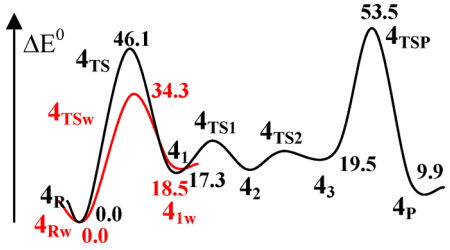

Figure 7. Schematic energy profile illustrating the process of formiminylation of 2-aminoacetonitrile. ΔE^0 is the zero-point energy corrected relative energy (in kcal/mol). Black is for the noncatalyzed reaction. Red is for the water-catalyzed process.

water molecule bridges the proton transfer during the reaction, the activation energy reduces to 34.3 kcal/mol for the formylation of 2-aminoacetonitrile. On the other hand, the examination of the energy profile along the reaction pathway indicates that the energy barrier of the dehydration process amounts to 34.0 kcal/mol. Thus, this reaction is energetically viable under the reported experimental conditions.[5]

5. Ring Closure: Formation of 5-Aminoimidazole. Ring-closure takes place in a process accompanied by a proton transfer from $-NH_2$ to $-CN$, forming an imidazoline compound (5-iminoimidazoline, Figure 8). Subsequently, a

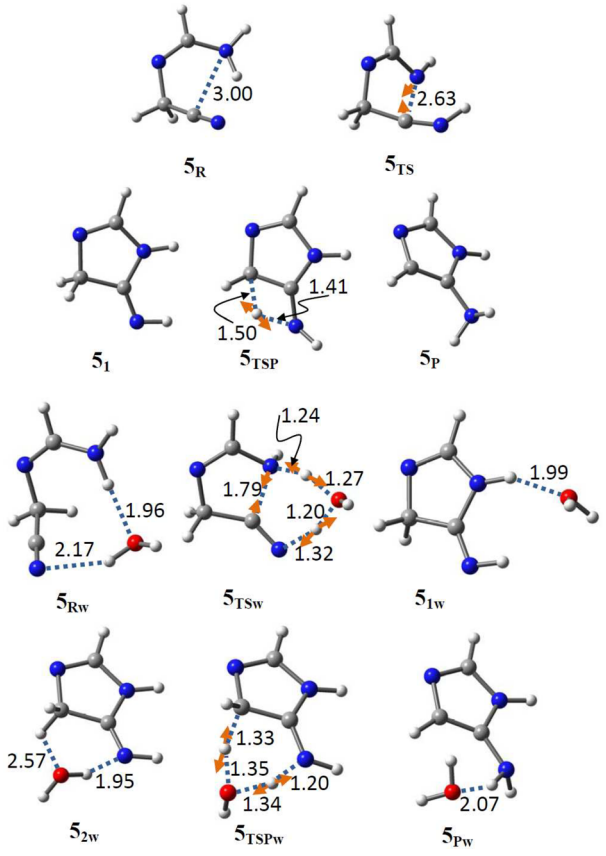

Figure 8. Optimized structures of the complexes as the local minima and the transition states on the PES in the process of five-membered ring-closure (Atomic distance in Å). Orange arrows represent the vibrational mode corresponding to the single imaginary frequency in the transition states. Color representations are: red for oxygen, blue for nitrogen, gray for carbon, and white for hydrogen.

proton migrates from the $-CH_2-$ at the 4-position of the imidazoline ring to the N atom of the imino group on the 5-position, yielding 5-aminoinidazole. In the absence of a water molecule, either ring-closure or intramolecular proton transfer is unlikely to happen due to the high energy barriers for both processes (57.8 kcal/mol for the former and 68.1 kcal/mol for the latter). However, in the presence of the dehydrated water and by proton-exchange through the water molecule, the activation energy of the ring-closing reduces to 41.9 kcal/mol. Moreover, due to the presence of a water molecule, the energy barrier corresponding to the intramolecular proton transfer reduces to 29.3 kcal/mol, as shown in the energy profiles of the reactions (Figure 9).

6. Formiminylation of 5-Aminoimidazole: Formation of (*Z*)-*N*′-(1*H*-Imidazol-5-yl)formamidine. Formylation of 5-aminoimidazole leads to the formation of an intermediate, (*S*)-(1*H*-imidazol-5-ylamino)(amino)methanol. In the successive dehydration process, the hydroxyl group attaches to the proton on the N atom of the secondary amino group at the 5-position of the imidazole group, yielding *N*′-(1*H*-imidazol-5-yl)formamidine (Figure 10). It should be noted that this N′-substituted formamidine species could possess either Z- or E-configurations. However, only the Z-isomer can lead to the

dx.doi.org/10.1021/jp311423q | J. Phys. Chem. B 2013, 117, 2314−2320

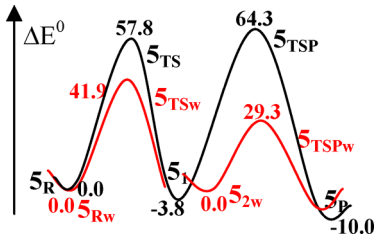

Figure 9. Energy profile along the reaction pathway of the process of ring-closure. ΔE^0 is the zero-point energy corrected relative energy (in kcal/mol). Black is for the noncatalyzed reaction. Red is for the water-catalyzed process.

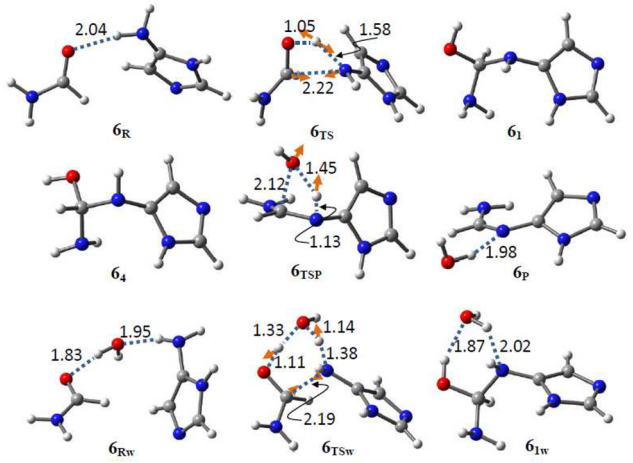

Figure 10. Optimized structures of the complexes as the local minima and the transition states on the PES in the formiminylation of 5-aminoimidazole (atomic distance in Å). Orange arrows represent the vibrational mode corresponding to the single imaginary frequency in the transition states. Color representations are: red for oxygen, blue for nitrogen, gray for carbon, and white for hydrogen.

formation of purine in the succeeding reactions. The energy barrier for the formylation of 5-aminoimidazole is evaluated to be 46.1 kcal/mol, and that for the dehydration process is calculated to be 34.3 kcal/mol. Figures 10 and 11 display the

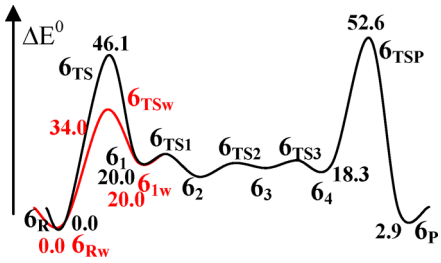

Figure 11. Energy profile along the reaction pathway of the process of the formiminylation of 5-aminoimidazole. ΔE^0 is the zero-point energy corrected relative energy (in kcal/mol). Black is for the noncatalyzed reaction. Red is for the water-catalyzed process.

energy profile and the structures of the intermediates and the transition states formed during the reactions leading to the formation of (*Z*)-*N*′-(1*H*-imidazol-5-yl)formamidine. In the presence of a water molecule, the activation energy of the formylation step is lowered to 34.0 kcal/mol.

7. Formiminylation of *N*′-(1*H*-Imidazol-5-yl)-formamidine: The Formation of (1*E*)-*N*′-((*Z*)-(1*H*-Imidazol-5-ylimino)methyl)formamidine. Formylation of *N*′-(1*H*-imidazol-5-yl)formamidine results in a formylated intermediate, (*Z*)-*N*-((*S*)-amino(hydroxy)methyl)-*N*′-(1*H*-imidazol-5-yl)formamidine (Figure 12). The subsequent dehydration

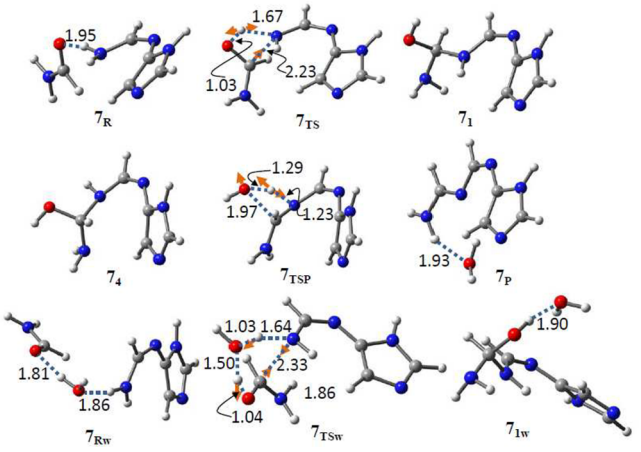

Figure 12. Optimized structures of the complexes as the local minima and the transition states on the PES in the formiminylation of *N*′-(1*H*-imidazol-5-yl)formamidine (atomic distance in Å). Orange arrows represent the vibrational mode corresponding to the single imaginary frequency in the transition states. Color representations are: red for oxygen, blue for nitrogen, gray for carbon, and white for hydrogen.

eliminates the hydroxyl group and the proton of the neighboring −NH− group, yielding the dehydrated compound, *N*′-((*Z*)-(1*H*-imidazol-5-ylimino)methyl)formamidine. Subsequent studies revealed that only the 1E-form is able to form the six-membered ring during the ring-closing reaction step. The energy profile along the reaction route (Figure 13) reveals

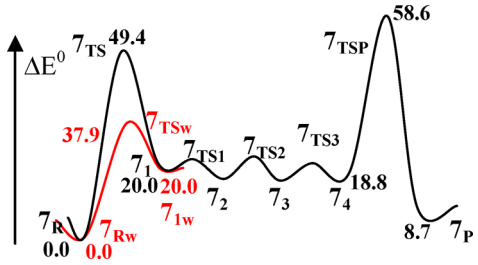

Figure 13. Energy profile along the reaction pathway. ΔE^0 is the zero-point energy corrected relative energy (in kcal/mol). Black is for the noncatalyzed reaction. Red is for the water-catalyzed process.

that the activation energy of the formylation step amounts to 49.4 kcal/mol, which is reduced to 37.9 kcal/mol when a water molecule serves as the proton transfer bridge. The energy barrier for the dehydration process is 39.8 kcal/mol, which is similar to those in the previous formiminylation reactions.

8. Six-Membered Ring Closure: Formation of Purine. Ring-closing takes place as the C—C single bond is formed between the C atom at 4-position of the imidazole group and the C atom of the formamidine. This process leads to the formation of (5*R*,6*S*)-6,9-dihydro-5*H*-purin-6-amine (Figure 14). A deamination reaction follows as 5H migrates to the amino group at the 6-position of the purine derivative, resulting in a purine molecule and an ammonia. Exploration of the detailed PES reveals that the energy barrier of the ring-closure

dx.doi.org/10.1021/jp311423q | J. Phys. Chem. B 2013, 117, 2314−2320

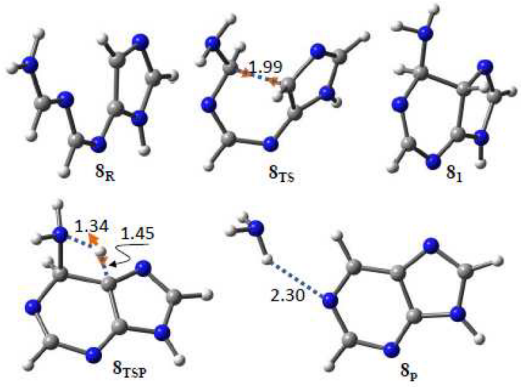

Figure 14. Optimized structures of the complexes as the local minima and the transition states on the PES in the ring-closure (atomic distance in Å). Orange arrows represent the vibrational mode corresponding to the single imaginary frequency in the transition states. Color representations are: blue for nitrogen, gray for carbon, and white for hydrogen.

step amounts to 32.2 kcal/mol and the energy barrier of deamination reaction amounts to 33.8 kcal/mol (Figure 15).

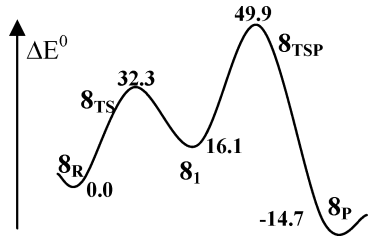

Figure 15. Energy profile along the reaction pathway of the six-membered ring-closure. ΔE^0 is the zero-point energy corrected relative energy (in kcal/mol).

DISCUSSIONS AND CONCLUSIONS

The step-by-step reaction pathway presented herein reveals the details of the mechanistic route of the transformation from formamide to purine, without the necessity of using any additional compounds. With the help of a water molecule, which is also a byproduct of the considered transformation, the highest energy barrier of the formation of HCN is around 34 kcal/mol. The hydrolysis of formamide that yields formate proceeds with an energy barrier less than 39 kcal/mol. Thus, all the compounds necessary for the reactions can be obtained during the studied transformations under relatively high temperature, such as near the boiling-point of formamide.

Several important reaction steps are involved in this mechanistic route: formylation-dehydration, Leuckart reduction, five-membered ring-closure, six-membered ring-closure, and deamination. Among these reactions, the Leuckart reduction and six-membered ring-closure processes are found to have energy barriers around 30 kcal/mol. The energy barrier for the deamination is slightly higher, 37 kcal/mol, as revealed in the present DFT study. These steps are expected to proceed at reasonable rates under the reported conditions.

Formylations in the considered reaction route are found to be energy demanding steps. The energy barriers of the formylations are around 50 kcal/mol. As concluded, these formylation steps could be sped up by including a water molecule during the reaction. With a water molecule enabling the proton transfer during the reaction, the activation barriers of formylation steps are found to be less than 38 kcal/mol. Energy barriers corresponding to the dehydration of the formylated products of the intermediates are revealed to be less than 40 kcal/mol. One exception is dehydration of 2-hydroxylaminoacetonitrile, for which the energy barrier amounts to 57 kcal/mol. Fortunately, this reaction can be sped up by the presence of a water molecule serving as a bridge for the proton transfer during the dehydration. In this case, the corresponding activation energy drops to less than 36 kcal/mol. It should be noted that the dehydration with a low energy barrier occurs between the hydroxyl group and the proton on the secondary amine, while the dehydration with a high energy barrier takes place on the primary amine. The proton on the secondary amine seems to be easily lost during the dehydration process.

These studies indicate that, as was revealed in previously reported studies,[19,20] the presence of catalytic water is critical for this reaction route. Without the presence of a water molecule, the five-membered ring-closure and the subsequent intramolecule proton transfer are unlikely to advance due to their high energy barriers (over 60 kcal/mol). Nevertheless, with water bridges, the proton transfer during these two reaction steps is governed by activation energy barriers reduced to 42 kcal/mol for the ring-closing step, and to 29 kcal/mol for the proton transfer step.

Overall, five-membered ring-closure is found to be the rate-determining step in the present mechanistic route. This is consistent with the longest reaction time (18 h) needed for this step in the experimental study.[5] The energy barrier of this rate-controlling step is somewhat lower than the rate-determination step (ca. 44 kcal/mol) in the pyrimidine path reported by Sponer et al.[20] The mechanistic pathway reported here is less energetically demanding than the formation of adenine through the pyrimidine route.

The highlight of the mechanistic route detailed herein is that this represents the simplest possible reaction system. All the reagents needed in the reaction can be acquired from one compound, formamide, through energetically viable pathways. Of course, the present study does not provide all answers. The feasibility of alternative mechanisms competing with this pathway requires further investigation. One of the particularly important tasks is the validation of various clusters with different numbers of explicit water molecules in the reaction pathways. These studies are currently being performed by our research group. Our work suggests one of the possible elucidations of the formation of purine from formamide and should provide useful information for exploring new and effective synthetic routes for the abiotic formation of nucleic acid bases and other biologically relevant molecules.

ASSOCIATED CONTENT

Supporting Information

Pathway about formation of formate through hydrolysis of formamide; structures of the intermediates and transition states for the reactions; table listing the enthalpies, free energies, and the SCF energies of all the structures in the studied pathways at B3LYP/6- 311G(d,p) level. This material is available free of charge via the Internet at http://pubs.acs.org.

dx.doi.org/10.1021/jp311423q | J. Phys. Chem. B 2013, 117, 2314−2320

AUTHOR INFORMATION

Corresponding Author

*E-mail: (J.G.) jiande@icnanotox.org; (J.L.) jerzy@icnanotox.org.

Notes

The authors declare no competing financial interest.

ACKNOWLEDGMENTS

This work was jointly supported by NSF and the NASA Astrobiology Program under the NSF Center for Chemical Evolution, CHE1004570. We would like to thank the Mississippi Center for Supercomputing Research for a generous allotment of computer time.

REFERENCES

(1) Gesteland, R. F., Cech, T., Atkins, J. F., Eds.; *The RNA World: The Nature of Modern RNA Suggests a Prebiotic RNA World*; Cold Spring Harbor monograph series; Cold Spring Harbor Laboratory Press: Cold Spring Harbor, NY, 2006.
(2) Miller, S. L., Orgel, L. E., Eds.; *The Origins of Life on Earth*; Prentice-Hall: Englewood Cliffs, NJ, 1974
(3) Schopf, J. W., Ed.; *Earth's Earliest Biosphere: Its Origin and Evolution*; Princeton University Press: Princeton, NJ, 1983.
(4) Saladino, R.; Crestini, C.; Ciciriello, F.; Costanzo, G.; Di Mauro, E. *Chem. Biodiversity* **2007**, *4*, 694−720.
(5) Hudson, J. S.; Eberle, J. F.; Vachhani, R. H.; Rogers, L. C.; Wade, J. H.; Krishnamurthy, R.; Springsteen, G. *Angew. Chem., Int. Ed.* **2012**, *51*, 5134−5137.
(6) Yamada, H.; Okamoto, T. *Chem. Pharm. Bull.* **1972**, *20*, 623−624.
(7) Bredereck, H.; Effenberger, F.; Rainer, G.; Schosser, H. P.; Liebigs, J. *Ann. Chem.* **1962**, *659*, 133−138.
(8) Nguyen, V. S.; Abbott, H. L.; Dawley, M. M.; Orlando, T. M.; Leszczynski, J.; Nguyen, M. T. *J. Phys. Chem. A* **2011**, *115*, 841−851.
(9) Saladino, R.; Crestini, C.; Costanzo, G.; Negri, R.; Mauro, E. D. *Bioorg. Med. Chem.* **2001**, *9*, 1249−1253.
(10) Saladino, R.; Ciamecchini, U.; Crestini, C.; Costanzo, G.; Negri, R.; Mauro, E. D. *ChemBioChem* **2003**, *4*, 514−521.
(11) Saladino, R.; Neri, V.; Crestini, C.; Costanzo, G.; Graciotti, M.; Mauro, E. D. *J. Am. Chem. Soc.* **2008**, *130*, 15512−15518.
(12) Saladino, R.; Crestini, C.; Costanzo, G.; Mauro, E. D. *Curr. Org. Chem.* **2004**, *8*, 1425−1433.
(13) Barks, H. L.; Buckley, R.; Grieves, G. A.; Mauro, E. D.; Hud, N. V.; Orlando, T. M. *ChemBioChem* **2010**, *11*, 1240−1243.
(14) Yamada, H.; Hirobe, M.; Higashiyama, K.; Takahashi, H.; Suzuki, K. T. *J. Am. Chem. Soc.* **1978**, *100*, 4617−4618.
(15) Ochiai, M.; Marumoto, R.; Kobayashi, S.; Shimazu, H.; Morita, K. *Tetrahedron* **1968**, *24*, 5731−5737.
(16) Yamada, H.; Hirobe, M.; Higashiyama, K.; Takahashi, H.; Suzuki, K. T. *Tetrahedron Lett.* **1978**, *19*, 4039−4042.
(17) Yamada, H.; Hirobe, M.; Okamoto, T. *Yakugaku Zasshi* **1980**, *100*, 489−492.
(18) Shuman, R. F.; Shearin, W. E.; Tull, R. J. *J. Org. Chem.* **1979**, *44*, 4532−4536.
(19) Roy, D.; Najafian, K.; Schleyer, P.; von, R. *Proc. Natl. Acad. Sci. U.S.A.* **2007**, *104*, 17272−17277.
(20) Sponer, J. E.; Mladek, A.; Sponer, J.; Fuentes-Cabrera, M. *J. Phys. Chem. A* **2012**, *116*, 720−726.
(21) Maeda, S.; Matsuda, Y.; Mizutani, S.; Fujii, A.; Ohno, K. *J. Phys. Chem. A* **2010**, *114*, 11896−11899.
(22) Wang, B.; Cao, Z. *J. Phys. Chem. A* **2010**, *114*, 12918−12927.
(23) Chaudhuri, C.; Jiang, J. C.; Wu, C.-C.; Wang, X.; Chang, H.-C. *J. Phys. Chem. A* **2001**, *105*, 8906−8915.
(24) Katsigiannis, C.; Mar, A.; Oró, J. *Origins Life Evol. Biospheres* **1986**, *16*, 297−298.
(25) Becke, A. D. *J. Chem. Phys.* **1993**, *98*, 5648−5652.
(26) Lee, C.; Yang, W.; Parr, R. G. *Phys. Rev. B* **1988**, *37*, 785−789.
(27) Miehlich, B.; Savin, A.; Stoll, H.; Preuss, H. *Chem. Phys. Lett.* **1989**, *157*, 200−206.
(28) Hehre, W. J.; Radom, L.; Schleyer, P. R.; Pople, J. A. *Ab Initio Molecular Orbital Theory*; Wiley: New York, 1986.
(29) Cossi, M.; Barone, V.; Cammi, R.; Tomasi, J. *Chem. Phys. Lett.* **1996**, *255*, 327−335.
(30) *Gaussian 09*, Revision A.1, Frisch, M. J.; Trucks, G. W.; Schlegel, H. B.; Scuseria, G. E.; Robb, M. A.; Cheeseman, J. R.; Scalmani, G.; Barone, V.; Mennucci, B.; Petersson, G. A.; Nakatsuji, H.; Caricato, M.; Li, X.; Hratchian, H. P.; Izmaylov, A. F.; Bloino, J.; Zheng, G.; Sonnenberg, J. L.; Hada, M.; Ehara, M.; Toyota, K.; Fukuda, R.; Hasegawa, J.; Ishida, M.; Nakajima, T.; Honda, Y.; Kitao, O.; Nakai, H.; Vreven, T.; Montgomery, J. A.; , Jr., Peralta, J. E.; Ogliaro, F.; Bearpark, M.; Heyd, J. J.; Brothers, E.; Kudin, K. N.; Staroverov, V. N.; Kobayashi, R.; Normand, J.; Raghavachari, K.; Rendell, A.; Burant, J. C.; Iyengar, S. S.; Tomasi, J.; Cossi, M.; Rega, N.; Millam, J. M.; Klene, M.; Knox, J. E.; Cross, J. B.; Bakken, V.; Adamo, C.; Jaramillo, J.; Gomperts, R.; Stratmann, R. E.; Yazyev, O.; Austin, A. J.; Cammi, R.; Pomelli, C.; Ochterski, J. W.; Martin, R. L.; Morokuma, K.; Zakrzewski, V. G.; Voth, G. A.; Salvador, P.; Dannenberg, J. J.; Dapprich, S.; Daniels, A. D.; Ö. Farkas, Foresman, J. B.; Ortiz, J. V.; Cioslowski, J.; Fox, D. J. Gaussian, Inc.: Wallingford, CT, 2009.
(31) Moore, M. L. In *Organic Reactions*; Adams, R., Bachmann, W. E., Blatt, A. H., Fieser, L. F., Johnson, J. R., Eds.; John Wiley and Sons: New York, 1949; Vol. *5*, pp 301−330.